Journal of Electrochemistry

Volume 11 | Issue 2

2005-05-28

A Preliminary Study of Electrocrystallization of Bismuth on Glassy Carbon

Min-li YANG

Zhan-jun ZHANG

Article ID: 1006-3471(2005)02-0133-07

A Preliminary Study of Electrocrystallization of Bismuth on Glassy Carbon

YANG Min-li, ZHANG Zhan-jun *

(College of Chemistry and Chemical Engineering, Graduate School, Chinese Academy of Sciences, Beijing 100049, China)

Abstract: The electrocrystallization of bismuth on glassy carbon electrodes (GCEs) from nitrate solutions was studied by cyclic voltammetry and chronoamperometry. Cyclic voltammograms exhibit a crossover between the cathodic and anodic branches, characteristic of the formation of bismuth nuclei on GCEs, and show that the bismuth electrocrystallization on GCEs is a diffusion-controlled reaction. The current transients were analyzed with the Scharifker and the Heerman equations. With the increase of Bi^{3+} concentration, the non-dimensional plots leaned to the theoretical curve for 3D instantaneous nucleation and growth. The overpotential dependence of nucleation and growth mechanism was also found. With the increase of overpotential, the non-dimensional curve approaches closer the limit for 3D instantaneous nucleation and growth. A quantitative analysis further shows that the nucleation rate constant (A) and the number density of active sites (N_0) exponentially grow with the increase of overpotential, and the diffusion coefficient (D) decays in an exponential mode, which was not reported before. A comparison between the kinetic parameter values obtained from the Scharifker equation and those from the Heerman equation was made, showing the very close N_0 and D values and the distinct A values (especially at - 300 and - 350 mV). However, under the experimental conditions of this work, both of the equations can be used for describing the electrocrystallization of bismuth on GCEs.

Key words: Electrocrystallization, Bismuth, Glassy carbon electrode, Nucleation, Growth, Scharifker equation, Heerman equation

CLC Number: O646 **Document code:** A

1 Introduction

Due to its unique physical and chemical properties, bismuth has been attracting many electrochemistry researchers. Most of the studies involving electrochemistry and bismuth can be divided into five classes: (a) a promising electrochromic material[1], (b) electrocatalytic activity of bismuth monolayer/submonolayer (underpotential deposition of bismuth) on some noble metal surfaces, as well as the effect of bismuth adatoms[2,3], (c) an attractive alternative to the traditionally used mercury film electrode in electroanalysis[4], (d) correlations between the morphologies and sizes of metallic bismuth with large magnetoresistance[5] or thermoelectric efficiency[6], and (e) overpotential deposition of bismuth onto several electrode materials[7,8]. It should be noted that, compared with the researches of the electrocrystallization of other metals such as copper, cobalt, and silver, the study of the mechanism of bismuth electrocrystal-

Received date: 2004-12-10, Accepted: 2005-01-29, * Corresponding author. Tel: (86-10) 88256331, E-mail: zhangzj@gscas.ac.cn
Support from the National Natural Science Foundation of China (20343003), and the Fund of President of the Graduate School of Chinese Academy of Sciences (GSCAS)

lization is very insufficient, and the growth mechanism of bismuth during bulk deposition is little understood[8,9], especially the early stages of electrocrystallization.

Electrochemical techniques such as cyclic voltammetry (CV) and chronoamperometry (CA) played a dual role: serving as the methods for metal deposition, and being used as diagnostic tools for the determination of reaction mechanisms[7]. To extract kinetic parameters from the experimental CA data, the Scharifker general equation[10] and the Heerman equation[11] were widely used. Milchev and Heerman[12] made a comment that, the Scharifker general equation underestimated the current at short times but described rigorously the long time, "Cottrell" behavior, whereas the Heerman equation predicted correct values for the current at short times but overestimated the current in the long time region. This paper will explore the mechanism of bismuth electrocrystallization on glassy carbon electrodes (GCEs) from nitrate solutions, and make a comparison between the Scharifker and the Heerman equations.

2 Experimental Section

2.1 Apparatus

Electrochemical measurements were performed with a CHI 440 electrochemical analyzer (CH Instruments), in connection with a personal computer. A GCE (3mm in diameter, CH Instruments, Austin, TX) served as the working electrode, with the Ag/AgCl (3 mol·L^{-1} KCl) electrode and platinum wire as the reference and counter electrodes, respectively. All potentials were given versus the Ag/AgCl (3 mol·L^{-1} KCl) electrode.

2.2 Chemicals and Reagents

All chemicals were of analytical grade. $Bi(NO_3)_3 \cdot 5H_2O$ was obtained from China Medicine (Group) Shanghai Chemical Reagent Corporation. Nitric acid (65%) was purchased from Beijing Beihua Fine Chemicals Co. Ltd. All solutions were prepared with deionized water produced by a Millipore system (Simplicity 185, Millipore).

2.3 Procedures

Prior to the electrochemical experiments, GCEs were hand-polished to a mirror-like finish with a slurry of alumina on Microcloth (Buehler), then cleaned in an ultrasonic bath of deionized water for 10 min and finally dried in a stream of nitrogen gas. Cyclic voltammetric measurements were performed at different scan rates. Chronoamperometric experiments were carried out by using a cathodic pulse from 0 mV to different deposition potentials from - 50 mV to - 500 mV. In order to clear out the residual metal, before the next measurement, a cleaning step was applied by holding the working electrode at + 500 mV for 2 min.

3 Results and Discussion

3.1 Cyclic Voltammetry Study

Fig. 1 shows the representative cyclic voltammogram for 20 mmol·L^{-1} Bi^{3+} /1 mol·L^{-1} HNO_3 obtained on GCEs at a scan rate of 500 mV/s. Potential scan started from + 500 mV, reversed at - 500 mV and terminated at + 500 mV. A couple of well-defined cathodic and anodic peaks and a crossover between the cathodic and anodic branches were observed clearly. The presence of the crossover is diagnostic for the formation of bismuth nuclei on GCEs.

In order to determine the type of control limiting the deposition process, besides the cyclic voltammograms for different Bi^{3+} concentrations obtained at 50

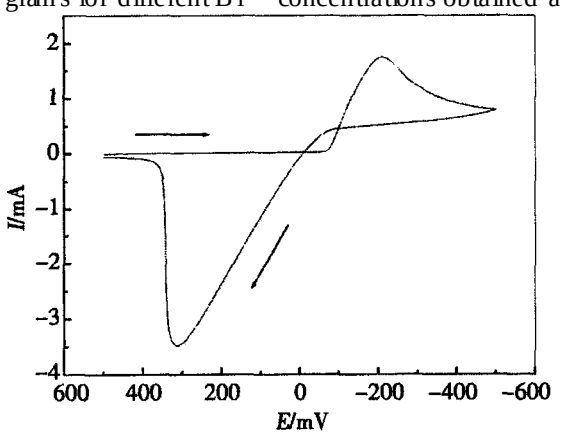

Fig. 1 Cyclic voltammogram for bismuth electrocrystallization onto glassy carbon electrodes from 20 mmol·L^{-1} Bi^{3+} /1 mol·L^{-1} HNO_3 at a scan rate of 500 mV/s

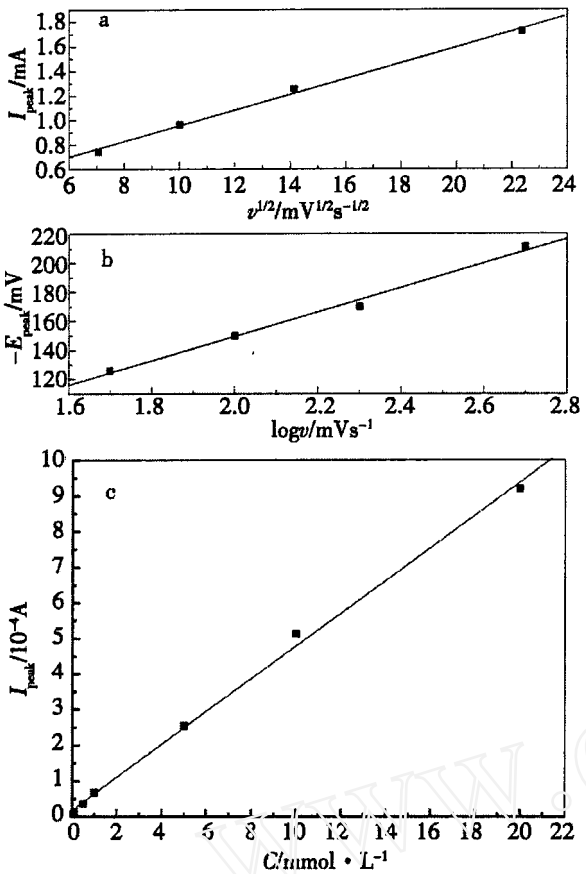

Fig 2　Plots of cathodic peak currents (I_{peak}) vs the square roots of the scan rates ($v^{1/2}$) (a, 20 mmol · L^{-1} Bi^{3+}), of cathodic peak potentials (E_{peak}) vs the logarithms of the scan rates (log v) (b, 20 mmol · L^{-1} Bi^{3+}), and of I_{peak} vs Bi^{3+} concentrations (c, 50 mV/s)

mV/s, a group of cyclic voltammograms for 20 mmol · L^{-1} Bi^{3+}/1 mmol · L^{-1} HNO_3 were recorded at different scan rates: 50, 100, 200, and 500 mV/s. Fig 2 presents the plot of the cathodic peak current (I_{peak}) vs the square root of scan rate ($v^{1/2}$), the plot of the cathodic peak potential (E_{peak}) vs the logarithm of scan rate (log v), and the plot of I_{peak} vs Bi^{3+} concentration. All the three plots exhibit an excellent linear relationship, which is characteristic of a diffusion-controlled reaction. The correlation coefficients (R) are respectively 0.997 7 for I_{peak} vs $v^{1/2}$, 0.998 8 for I_{peak} vs Bi^{3+} concentration, and 0.995 6 for E_{peak} vs log v.

3.2　Chronoamperometry Study

Chronoamperometry is a very important diagnostic electrochemical technique for electrocrystallization studies. It is well known that Scharifker and Hills[14] developed the model for the three-dimensional (3D) multiple nucleation with diffusion-controlled growth.

The expressions for instantaneous and progressive nucleation with 3D growth are given by Eq. (1) and Eq. (2), respectively.

$$\frac{I^2}{I_{max}^2} = \frac{1.9542}{t/t_{max}}\{1 - \exp[-1.2564(t/t_{max})]\}^2 \quad (1)$$

$$\frac{I^2}{I_{max}^2} = \frac{1.2254}{t/t_{max}}\{1 - \exp[-2.3367(t/t_{max})^2]\}^2 \quad (2)$$

where I_{max} and t_{max} are the current and time coordinates of the chronoamperometric peak. The two equations provide a convenient criterion for distinguishing between these two extreme cases of nucleation kinetics.

Fig 3 is the non-dimensional I^2/I_{max}^2 vs t/t_{max} plots of the data for bismuth electrocrystallization onto GCEs from 1 mol · L^{-1} HNO_3 solutions containing 20, and 10 mmol · L^{-1} Bi^{3+}, where the solid and dotted lines are the theoretical transients respectively for 3D instantaneous and progressive nucleation with diffusion-controlled growth. The effect of Bi^{3+} concentration on nucleation and growth mechanisms can be observed from Fig 3. With the increase of Bi^{3+} concentration, the non-dimensional plots lean to the theoretical curve for 3D instantaneous nucleation and growth, suggesting high concentration is helpful for the formation of dense and uniform Bi deposits. Also, the plots corresponding to 20 and 10 mmol · L^{-1} Bi^{3+} show a potential dependence of nucleation and growth mechanism. With the increase of overpotential, the non-dimensional curve approaches closer the limit for 3D instantaneous nucleation and growth. Such a potential dependence was also found in the electrocrystallization of copper on Au(111)[15], silver on different carbon substrates[16], and bismuth on fluorine-doped tin oxide-coated conducting glass substrates[17].

For a further analysis of the kinetics mechanism shown by Fig 3, a general equation should be used as

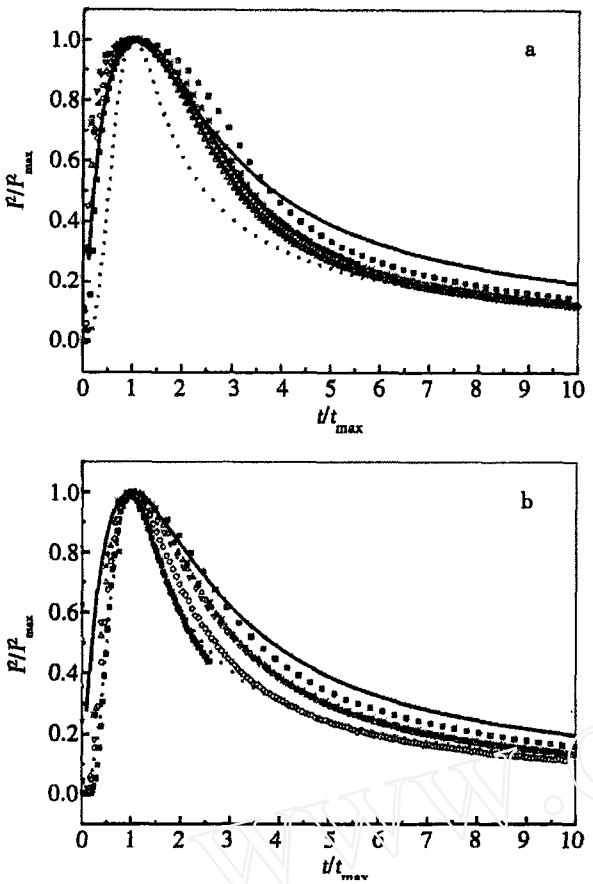

Fig 3 Non-dimensional I^2/I^2_{max} vs t/t_{max} plots of the data for bismuth electrocrystallization onto glassy carbon electrodes from 1 mol · L^{-1} HNO_3 solutions containing (a) 20 and (b) 10 mmol · L^{-1} Bi^{3+} the electrode potential was stepped from 0 mV to ■) - 100, ○) - 150, △) - 200, ▽) - 250, *) - 300, and ⊙) - 350 mV. The theoretical transients for instantaneous (solid line) and progressive (dotted line) nucleation were calculated according to the Scharifker-Hills model

the theoretical model for the estimation of typical kinetics parameters, nucleation rate constant (A) and number density of active sites (N_0). Often used is the Scharifker's general equation[10] i e

$$I_{3D-DC}(t) = \frac{zFD^{1/2}C}{\pi^{1/2}t^{1/2}}[1 - \exp(-N_0\pi k'Dt\theta)] \quad (3)$$

with

$$\theta = 1 - \frac{(1 - \exp(-At))}{At} \quad (4)$$

where zF is the molar charge transferred during electrocrystallization, D is the diffusion coefficient, C is the bulk concentration of the electroactive species, t is time. The k' is defined by Equation 4, of which M and ρ are the atomic weight and the density of the deposit, respectively.

$$k' = \frac{4}{3}\left(\frac{8\pi CM}{\rho}\right)^{1/2} \quad (5)$$

It should be noted that Heerman and Tarallo[11] proposed a modification to the Scharifker general equation:

$$I_{3D-DC}(t) = \frac{\Phi}{\theta}\frac{zFD^{1/2}C}{\pi^{1/2}t^{1/2}}[1 - \exp(-N_0\pi k'Dt\theta)] \quad (6)$$

where

$$\Phi = 1 - \frac{\exp(-At)}{(At)^{1/2}}\int_0^{(At)^{1/2}} \exp(\lambda^2)\,d\lambda \quad (7)$$

Since the function $F(x) = \exp(-x^2)\int_0^x \exp(\lambda^2)\,d\lambda$ can be efficiently approximated with the polynomial[17]

$$F(x) = \frac{0.051314213 + 0.47910725x}{1 - 1.2068142x + 1.185724x^2} \quad (8)$$

Eq. (7) can be rewritten as

$$\Phi = \frac{a - 1.2068142A^{1/2}t^{-1/2} + 1.185724At - 0.051314213A^{-1/2}t^{-1/2}}{1 - 1.2068142A^{1/2}t^{1/2} + 1.185724At}$$

$$a = 0.52089275 \quad (9)$$

The nonlinear parameter estimation was done by fitting Eq. (3) and Eq. (6) to the experimental data points. A commercial software based on the Levenberg-Marquardt algorithm served as the tool for the nonlinear fitting. Six groups of original experimental current transients obtained at six different deposition potentials (corresponding to Fig. 3a) were analyzed. The best-fit kinetics parameters, A, N_0, and D, were listed in Tab. 1. Fig. 4 shows a very clear potential dependence of A, N_0, and D. Whichever model was used, A and N_0 exponentially grew with the increase of overpotential, while D decayed in an exponential mode. Similar phenomenon was described by Palomar-Pardave etc. in their study of copper OPD onto Au(111)[15].

Also, Fig. 4 provides a direct comparison between the kinetic parameter values obtained from the Scharifker equation and those from the Heerman equation. It can be observed that, the two equations resulted in the very close N_0 and D values and the distinct A values (especially at - 300 and - 350

Tab. 1　Kinetic parameters of the bismuth OPD from 20 mmol · L^{-1} Bi^{3+} /1 mol · L^{-1} HNO_3 onto GCEs. Estimated by using Eq. (3), Scharifker equation and Eq. (6), Heerman equation

- E/mV	Scharifker equation			Heerman equation		
	$A/10^4$ s^{-1}	$N_0/10^7$ cm^{-2}	$D/10^{-6}$ $cm^2 \cdot s^{-1}$	$A/10^4$ s^{-1}	$N_0/10^7$ cm^{-2}	$D/10^{-6}$ $cm^2 \cdot s^{-1}$
100	0.00551	0.16458	11.06950	0.00414	0.16007	10.72400
150	0.03130	0.48550	9.90971	0.01964	0.48060	9.76009
200	0.19931	1.26003	9.26057	0.09633	1.26141	9.19914
250	0.84059	2.29023	9.01560	0.31255	2.29961	8.98446
300	3.79127	4.04106	8.78891	0.68042	4.08380	8.76411
350	10.77039	6.46130	8.67057	1.14466	6.53903	8.64899

Tab. 2　Linear fitting parameters for the plot of ln$A$ vs E and the estimated N_c (critical nucleus size)

Models	Section 1			Section 2		
	R	Slope	N_c	R	Slope	N_c
Scharifker Equation	0.998 75	33.869 29	0	0.994 57	25.504 55	0
Heerman Equation	0.997 84	29.122 34	0	0.993 49	12.980 96	0

mV). According to the atomistic theory of electrolytic nucleation, the critical size of the nuclei (N_c) can be estimated using Eq. (10).

$$N_c = \frac{KT}{ze_0}\left(\frac{-\mathrm{d}lnA}{\mathrm{d}E}\right) - \alpha \qquad (10)$$

where K is the Boltzmann constant, T is the absolute temperature, z is the number of electrons transferred during the electrochemical reaction, e_0 is the elementary electric charge, and α is the kinetic transfer coefficient.

With an attempt to judge the kinetic parameter values obtained from the two equations, ln$A$ was plotted as a function of - E (shown in Fig. 5). It has been shown that, the ln$A$ vs - E curve should be represented by a cusped line, each sector corresponding to a given number of atoms. Each plot in Fig. 5 contains two sections of different slopes. From the slopes and using a transfer coefficient value of 0.5 and a temperature of 298 K, N_c values were estimated by Eq. (10) (see Tab. 2). The result N_c = 0 means that, within the investigated potential interval, the single adsorbed bismuth atoms are strongly bounded with GCE surface and form the stable one-atomic "clusters" that can grow irreversibly at the applied potential. Such a phenomenon was ever reported in the electrocrystallization of rhodium on polycrystalline gold[19]. These results suggested that, both the Scharifker and the Heerman equations can be used for describing the electrocrystallization of bismuth on GCEs, at least under the experimental conditions of this work.

4　Conclusions

Cyclic voltammograms for bismuth electrocrystallization on GCEs from nitrate solutions showed a couple of well-defined cathodic and anodic peaks and a crossover between the cathodic and anodic branches. The further analysis indicated that the electrocrystallization of bismuth on GCEs is a diffusion-controlled reaction.

The experimental current transients were analyzed with the Scharifker equation and the Heerman equation. With the increase of Bi^{3+} concentration, the non-dimensional plots leaned to the theoretical curve for 3D instantaneous nucleation and growth, suggesting high concentration was helpful for the formation of dense and uniform Bi deposits. In the cases of 10 and 20 mmol · L^{-1} Bi^{3+}, a potential dependence of nucleation and growth mechanism was also be found. With the increase of overpotential, the non-di-

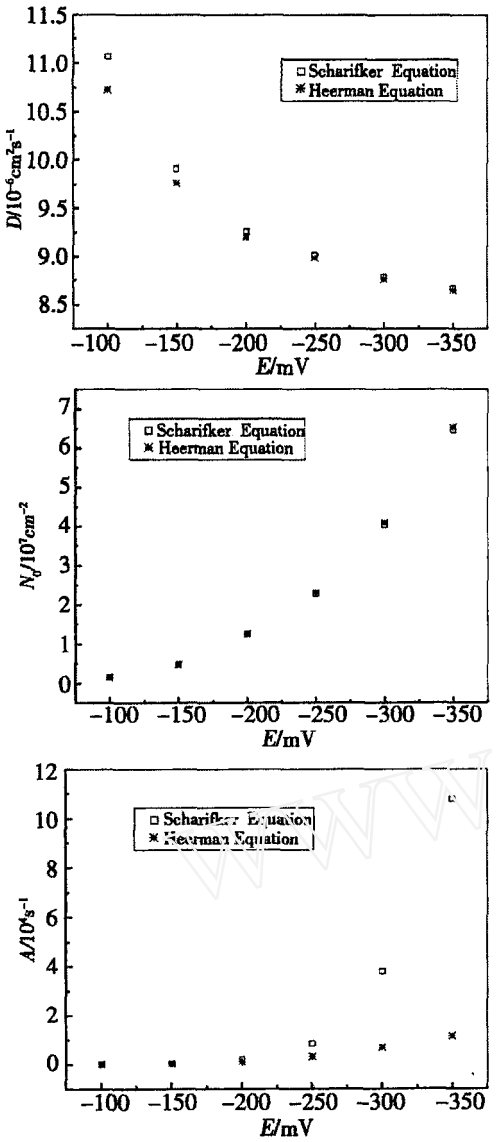

Fig 4 Plots of typical kinetics parameters in Table 1 vs deposition potentials. A, N_0, and D denote the nucleation rate constant, the number density of active sites, and the diffusion coefficient, respectively

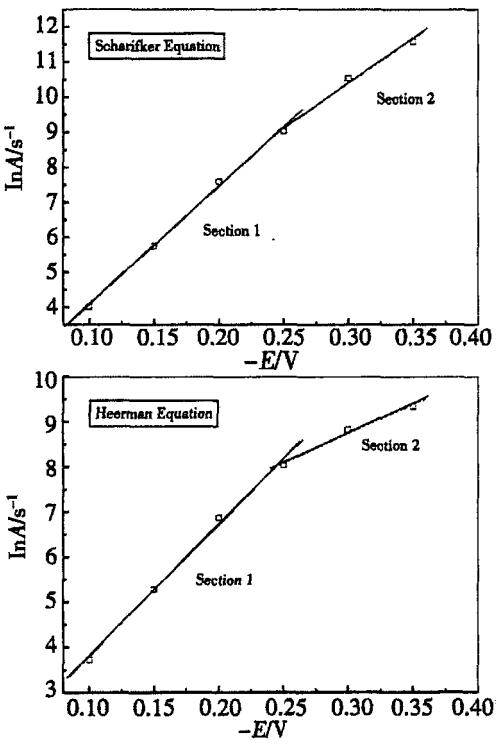

Fig 5 Variation of the ln$A$ with electrode potential for bismuth OPD onto GCEs from 20 mmol · L^{-1} Bi^{3+} / 1 mol · L^{-1} HNO_3
the A values (nucleation rate) were obtained from (upper) Eq. (3) and (lower) Eq. (6), respectively

mensional curve approaches closer the limit for 3D instantaneous nucleation and growth. A quantitative analysis further showed that A and N_0 exponentially grew with the increase of overpotential, while D decayed in an exponential mode.

The kinetic parameter values such as N_0 and D obtained from the Scharifker equation were very close to those from the Heerman equation, while there were differences between the two groups of A values (especially at - 300 and - 350 mV). Under the experimental conditions of this work, both of the equations can be used for describing the electrocrystallization of bismuth on GCEs from nitrate solutions. It was shown that, within the investigated potential interval, the single adsorbed bismuth atoms could be strongly bounded with GCE surface and formed the stable one-atomic "clusters" that could grow irreversibly at the applied potential.

Acknowledgments: M. Yang thanks the supervision of Prof. Hu Zhongbo from College of Chemistry and Chemical Engineering of GSCAS, and is also grateful to Prof. B. Scharifker for the helpful advice.

References:

[1] Ziegler J P. Status of reversible electrodeposition electrochromic devices [J]. Solar Energy Materials & Solar Cells, 1999, 56: 477.

[2] Ben Aoun S, Dursun Z, Sotomura T, et al. Effect of metal ad-layers on Au(111) electrodes on electrocatalytic reduction of oxygen in an alkaline solution [J]. Electrochemistry Communications, 2004, 6: 747.

[3] Tamura K, Wang J X, Adzic R R, et al. Kinetics of monolayer Bi electrodeposition on Au(111): surface X-ray scattering and current transients [J]. J. Phys. Chem. B, 2004, 108: 1 992.

[4] Kruusma J, Banks C E, Compton R G. Mercury-free sono-electroanalytical detection of lead in human blood by use of bismuth-film-modified boron-doped diamond electrodes [J]. Anal Bioanal Chem., 2004, 379: 700.

[5] Jiang S, Huang Y, Luo F, et al. Synthesis of bismuth with various morphologies by electrodeposition [J]. Inorganic Chemistry Communications, 2003, 6: 781.

[6] Li L, Zhang Y, Li G, et al. A route to fabricate single crystalline bismuth nanowire arrays with different diameters [J]. Chemical physics Letters, 2003, 378: 244.

[7] Sadale S B, Patil P S. Nucleation and growth of bismuth thin films onto fluorine-doped tin oxide-coated conducting glass substrates from nitrate solutions [J]. Solid state Ionics, 2004, 167: 273.

[8] Jeffrey C A, Harrington D A, Morin S. In situ scanning tunneling microscopy of bismuth electrodeposition on Au(111) surfaces [J]. Surface Science, 2002, 512: L 367.

[9] Solomun T, Kautek W. Electrodeposition of bismuth and silver phases in nanometer-sized zero-dimensional STM-formed cavities on gold(111) [J]. Electrochimica Acta, 2001, 47: 679.

[10] Scharifker B R, Mostany J. Three-dimensional nucleation with diffusion controlled growth: Part I. Number density of active sites and nucleation rates per site [J]. J. Electroanal Chem., 1984, 177: 13.

[11] Heerman L, Tarallo A. Theory of the chronoamperometric transient for electrochemical nucleation with diffusion-controlled growth [J]. J. Electroanal Chem., 1999, 470: 70.

[12] Milchev A, Heerman L. Electrochemical nucleation and growth of nano- and microparticles: some theoretical and experimental aspects [J]. Electrochimica Acta, 2003, 48: 2 903.

[13] Berzins T, Delahay P. Oscillographic polarographic waves for the reversible deposition of metals on solid electrodes [J]. J. Am. Chem. Soc., 1953, 75: 555.

[14] Scharifker B, Hills G. Theoretical and experimental studies of multiple nucleation [J]. Electrochimica Acta, 1983, 28: 879.

[15] Palomar-Pardave M, Gonzalez I, Batina N. New insights into evaluation of kinetic parameters for potentiostatic metal deposition with underpotential and overpotential Deposition processes [J]. J. Phys. Chem. B, 2000, 104: 3 545.

[16] Miranda-Hernandez M, Gonzalez I, Batina N. Silver electrocrystallization onto carbon electrodes with different surface morphology: active sites vs surface features [J]. J. Phys. Chem. B, 2001, 105: 4 214.

[17] Heerman L, Tarallo A. Electrochemical nucleation on microelectrodes. Theory and experiment for diffusion-controlled growth [J]. J. Electroanal. Chem., 1998, 451: 101.

[18] Budevski E, Staikov G, Lorenz W J. Eletrocrystallization nucleation and growth phenomena [J]. Electrochimica Acta, 2000, 45: 2 559.

[19] Arbib M, Zhang B, Lazarov V, et al. Electrochemical nucleation and growth of rhodium on gold substrates [J]. J. Electroanal. Chem., 2001, 510: 67.

铋在玻碳电极上电化学结晶初步研究

杨民力,张占军*

(中国科学院研究生院,化学与化工学院,北京, 100049)

摘要: 应用循环伏安法和计时安培法研究了铋在玻碳电极上的电结晶行为. 循环伏安曲线显示了铋在玻碳电极上成核的典型特征,并表明其于玻碳电极上的电结晶是一个扩散控制过程. 根据计时安培法响应曲线分析阐明了铋的浓度和过电势对成核生长机理的影响. 进一步的定量测试表明该成核速率常数 A 和活化点密度 N_0 随过电势增加呈现指数增大规律;扩散系数 D 随过电势增加呈指数衰减. 以上实验结果至今未见报道. 同时表明: Scharifker公式和 Heerman公式均可用于本实验的理论解释.

关键词: 电结晶;铋;玻碳电极;成核;生长; Scharifker公式; Heerman公式